Near-Ocean Bottom Wavefield Tomography for Elastic Wavefield Decomposition

*Ali M. Alfaraj *, D.J. Verschuur, and Kees Wapenaar, Delft University of Technology.*

Summary

The use of multi-component ocean bottom data becomes more popular; however, for accurate quantitative imaging proper decomposition in upgoing P- and S-waves is required. Elastic wavefield decomposition at the ocean bottom requires properties of the ocean floor in order to get reliable one-way wavefields, which is complicated by the fact that these properties can vary considerably close to the bottom. We consider the situation that via the JMI process, (Joint Migration Inversion), an estimate for the up-going P- and S-waves at a certain depth level below the ocean bottom has been obtained. We develop an inversion scheme that estimates the P- and S-wave velocities in the remaining part of the subsurface, between the depth level below the water bottom and the bottom itself. In addition, we apply a composition of the resulting up-going wavefields at the bottom into the measured quantities by the 4-C receivers. Thus, a combined tomography and decomposition problem is solved. In this way, the unknown properties of the ocean bottom as well as the velocities in the near bottom layer are estimated based on comparing the predicted data with the true measurements. Results indicate that it is possible to develop an inversion scheme that estimates the near-bottom velocity model in combination with the optimum decomposition operators.

Introduction

For exploiting the rich information in multicomponent measurements at the ocean bottom, it is required to perform elastic wavefield decomposition in order to have pure P- and S-wave records. The reliability of any further processing of the seismic data depends on whether the decomposed data can be obtained with high accuracy. Elastic wavefield decomposition just below the ocean bottom requires the properties of the first layer beneath the receivers, however, this layer can have quite strong variations in the elastic properties. One of the current practice methods for estimating the near-bottom parameters is via refraction tomography surveys, which are based on first-break picking. For large data sets, this method is time consuming. (Schalkwijk et al., 2003) suggested an adaptive wavefield decomposition scheme, with which the near-ocean bottom parameters can be estimated, and applied it to field data as well. This approach allows good decomposition results. However, it is based on different criteria that require direct arrivals picking and events identification.

We perform wavefield tomography to build P- and S-wave velocity models of the near-ocean bottom layers. Berkhout (2012) proposed the Joint Migration Inversion scheme, which aims at estimating the velocity and reflectivity. Full wavefield tomography is the part of JMI that estimates the velocities. This approach is data-driven and capable of utilizing the total wavefield including all multiples and transmission effects. It does not require first arrival picking as in travel time tomography, but rather finds a distribution of velocities and reflections such that the two-way modeled wavefield matches the observed data. The methodology was further described by Berkhout (2014) and implemented by Staal and Verschuur (2013), Staal et al. (2014) and Alshuhail et al. (2014) on acoustic pressure data. We assume that via the JMI method (or another approach), we have obtained the up-going P- and S- wavefields at a known depth in the vicinity of the water bottom (e.g. few 100 meters below the bottom) and our task is to find the velocities of the layers between this depth and the bottom. With those estimated velocities, we compose the up-going P- and S-waves to form the modeled vertical and horizontal velocity components which can then be matched with the measurements. Since composition requires the down-going P- and S-waves as well, we express them in terms of the acoustic pressure measurement. At the end, we test the sensitivity of elastic decomposition to the ocean floor velocities. Although we finally aim for a multi-dimensional implementation, in this study we restrict ourselves to a 1,5D situation, such that all equations are presented in the rayparameter - frequency domain.

Theory

Following the work of Wapenaar and Berkhout (1989) and Wapenaar et al. (1990), we briefly review the theory of elastic wavefield decomposition. We consider a horizontally layered medium where medium parameters vary with respect to depth only. To reach to an expression for the decomposed up- and down-going wavefields, we need the established relationship between the recorded two-way wavefields ($\widetilde{\boldsymbol{Q}}$) and the desired one-way wavefields ($\widetilde{\boldsymbol{D}}$). They are related by the composition ($\widetilde{\boldsymbol{L}}$) and decomposition $\widetilde{\boldsymbol{N}}$ matrices such that

$$\widetilde{\boldsymbol{Q}}(z) = \widetilde{\boldsymbol{L}}(z)\widetilde{\boldsymbol{D}}(z) \quad \text{and} \qquad (1a)$$
$$\widetilde{\boldsymbol{D}}(z) = \widetilde{\boldsymbol{L}}^{-1}(z)\widetilde{\boldsymbol{Q}}(z) = \widetilde{\boldsymbol{N}}(z)\widetilde{\boldsymbol{Q}}(z). \qquad (1b)$$

For the elastic case, $\widetilde{\boldsymbol{Q}}$ contains the traction ($\widetilde{\boldsymbol{T}}$) and the particle velocity ($\widetilde{\boldsymbol{V}}$) while $\widetilde{\boldsymbol{D}}$ is chosen to be the P- and S-wave potentials ($\widetilde{\boldsymbol{\Phi}}$) and ($\widetilde{\boldsymbol{\Psi}}$), respectively. At the ocean bottom ($z = z_1$), figure 1, the shear tractions vanish, $\tau_{xz}(z_1) = \tau_{yz}(z_1) = 0$, and the negative of the normal traction is equivalent to the acoustic pressure, $-\tau_{zz}(z_1) = p(z_1)$. We consider waves that are polarized in the $(x - z)$ plane. We also neglect SH waves and take into account only

Wavefield Tomography for Elastic Decomposition

P-SV waves. The composition and decomposition equations become

$$\begin{pmatrix} -\tilde{T}_{xz}(z_1) \\ -\tilde{T}_{zz}(z_1) \\ \tilde{V}_x(z_1) \\ \tilde{V}_z(z_1) \end{pmatrix} = \begin{pmatrix} \tilde{\mathbf{L}}_{1,p-sv}^+(z_1) & \tilde{\mathbf{L}}_{1,p-sv}^-(z_1) \\ \tilde{\mathbf{L}}_{2,p-sv}^+(z_1) & \tilde{\mathbf{L}}_{2,p-sv}^-(z_1) \end{pmatrix} \begin{pmatrix} \Phi^+(z_1) \\ \Psi_y^+(z_1) \\ \Phi^-(z_1) \\ \tilde{\Psi}_y^-(z_1) \end{pmatrix} \quad (2a)$$

and

$$\begin{pmatrix} \Phi^+(z_1) \\ \Psi_y^+(z_1) \\ \tilde{\Phi}^-(z_1) \\ \tilde{\Psi}_y^-(z_1) \end{pmatrix} = \begin{pmatrix} \tilde{\mathbf{N}}_{1,p-sv}^+(z_1) & \tilde{\mathbf{N}}_{2,p-sv}^+(z_1) \\ \tilde{\mathbf{N}}_{1,p-sv}^-(z_1) & \tilde{\mathbf{N}}_{2,p-sv}^-(z_1) \end{pmatrix} \begin{pmatrix} -\tilde{T}_{xz}(z_1) \\ -\tilde{T}_{zz}(z_1) \\ \tilde{V}_x(z_1) \\ \tilde{V}_z(z_1) \end{pmatrix}. \quad (2b)$$

Since elastic decomposition is performed just below the ocean bottom, the composition and decomposition operators are dependent on the properties of the first layer beneath the receivers, $\rho(z_1)$, $c_p(z_1)$ and $c_s(z_1)$. In order to find $c_p(z_1)$ and $c_s(z_1)$, we perform wavefield tomography.
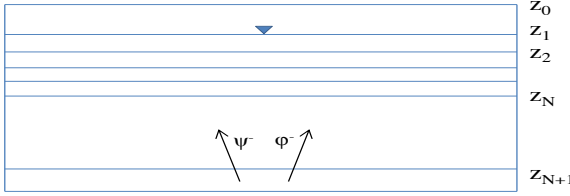

Figure 1: Illustration of depth levels

We present the theory of wavefield tomography, which is the part of JMI that estimates the velocity, as proposed by Berkhout (2012) and Staal and Verschuur (2013). If the wavefield propagates between two levels, z_n and z_m, in two different velocity models, it will experience two different extrapolation effects. Assume that the velocity models form the true and the background velocity model, with their corresponding extrapolation operators W^- and W_0^-, respectively. The expression of the true extrapolation operator in terms of the background extrapolation operator reads

$$W^-(z_m, z_n) = W_0^-(z_m, z_n) + \Delta W^-(z_m, z_n). \quad (3)$$

These extrapolation operators are phase shift operators expressed in the frequency-rayparameter domain as:

$$\tilde{W}^-(p, z_m, z_n, \omega) = e^{-j\omega q \Delta z}, \quad (4a)$$

where q is dependent on the rayparameter p and on the propagation velocity. This means it is different for P- or S-wave propagation:

$$q_p = \sqrt{\frac{1}{c_p^2} - p^2}, \quad q_s = \sqrt{\frac{1}{c_s^2} - p^2}. \quad (4b)$$

We define β to be the P- and S-wave velocity contrasts at each depth level

$$\beta_p(z) = 1 - \frac{c_{p0}(z)^2}{c_p(z)^2}, \qquad \beta_s(z) = 1 - \frac{c_{s0}(z)^2}{c_s(z)^2}. \quad (5)$$

Performing Taylor series expansion for $\tilde{W}$ at $\beta = 0$ and ignoring higher order terms results in (see also Sava and Biondi, 2004):

$$\Delta \tilde{W}^-(z_m, z_n) \approx G_0^-(z_m, z_n)\beta(z), \quad (6a)$$

with

$$G_0^-(z_m, z_n) = j\omega\Delta z \frac{q_0^2}{2q} e^{-j\omega q \Delta z}, \quad (6b)$$

$$q = \sqrt{q_0^2(1 - \beta(z)) - p^2} \text{ and } q_0 = \frac{1}{c^2}. \quad (6c)$$

From equations (3) and (6), it can be seen that it is possible to retrieve the true extrapolation operator from the known background extrapolation operator and the linearized difference extrapolation operator.

We define $\tilde{Q}_p^-(z_n)$ and $\tilde{Q}_s^-(z_n)$ to be the up-going wavefields at a certain depth level (z_n). These are the assumed-known $\tilde{\Phi}^-(z_{N+1})$ and $\tilde{\Psi}_y^-(z_{N+1})$, forward extrapolated with $\tilde{W}_0^-(z_n, z_{N+1})$, figure 1. This is just an assumption to reduce the wavefield tomography to a subset of a larger scheme, in which the up-going wavefields are actually estimated. In the rest of this paper, we will only present the equations for the S-wave. P-wave equations are similar.

The cumulative effect of the velocity perturbations from all the depth levels on the up-going wavefields recorded at the ocean bottom (z_1) are given by:

$$\Delta \tilde{\Psi}(z_1) = \sum_{n=2}^{N} \underline{\tilde{G}}_{s0}^-(z_1, z_n)\,\beta_s(z_n)\tilde{Q}_s^-(z_n), \quad (7a)$$

where

$$\underline{\tilde{G}}_{s0}^-(z_1, z_n) = \tilde{W}_{s0}^-(z_1, z_{n-1})\tilde{G}_{s0}^-(z_{n-1}, z_n) \quad (7b)$$

and

$$\tilde{Q}_s^-(z_n) = \tilde{W}_{s0}^-(z_n, z_{N+1})\tilde{\Psi}_y^-(z_{N+1}). \quad (7c)$$

Assume that there is a velocity contrast β between the background and the true velocity models, then equation (7) can predict the difference between the two wavefields propagating in each model. This estimated residual might be different from the actual residual in the case that the true wavefield experience multiple reflections that are not experienced by the estimated wavefield. This is because the estimated wavefield takes into account only transmission effects.

Wavefield Tomography for Elastic Decomposition

Inversion for near-ocean bottom velocities

The objective function and the corresponding gradient are:

$$J_s = \sum_{p_1}^{p_2} \sum_{\omega_1}^{\omega_2} ||\widetilde{\Psi}_{obs}^-(z_1) - \widetilde{\Psi}_{mod}^-(z_1)||^2 \qquad (8a)$$

and

$$\nabla\beta_s(z_n) = \sum_{p_1}^{p_2} 2[\tilde{\underline{G}}_{s_0}^-(z_n, z_1)]^* \Delta\widetilde{\Psi}^-(z_1)[\tilde{Q}_s^-(z_n)]^*. \qquad (8b)$$

Note that $\nabla\beta_s(z_n)$ contains the velocity contrasts based on wavefields that propagate with a range of p values. The angle-dependent contributions at a certain depth level are combined to result in one $\nabla\beta_s(z_n)$ describing the velocity variations as a function of depth.

Using the computed gradients, we predict the wavefield perturbations for each p value with

$$\Delta\Psi_{\nabla\beta_s}^-(z_1) = \sum_{n=2}^{N} \tilde{\underline{G}}_{s_0}^-(z_1, z_n)\nabla\beta_s(z_n)\tilde{Q}_s^-(z_n). \qquad (9)$$

Now, we can update the velocity contrasts β and the velocities as follows:

$$\beta_s(z)^{new} = \beta_s(z)^{old} + \alpha_s\nabla\beta_s(z) \text{ and} \qquad (10a)$$

$$c_s(z)^{new} = \frac{c_s(z)^{old}}{\sqrt{1 - \alpha_s\nabla\beta_s(z)}}. \qquad (10b)$$

Numerical example

To test the wavefield tomography method, we applied it to synthetic multi-component ocean bottom data. The data is modeled in the tau-p domain considering a 1.5D elastic model. In this domain, each slowness value (p) corresponds to a certain angle of propagation of a plane wave. Results before and after applying wavefield tomography are shown in figures 2-4. Due to cycle skipping in the S-wave inversion, we applied multi-scale inversion. We performed 10 iterations at each of the following frequency bandwidths: $(5 - 8)$, $(5 - 20)$, $(5 - 60)$ Hz. The retrieved velocity models are smooth representations of the true velocities, as we only take into account transmission effects.

Wavefield composition

Using equation (2a), we can compose the modeled two-way horizontal and vertical velocity components, which require the four potentials and the ocean floor parameters. For the sake of simplicity, we assume a known density profile. Since we only updated the up-going potentials in the tomography process, we express the down-going potentials in terms of

the vanishing shear traction and the observed acoustic pressure to get:

$$\widetilde{\Psi}^+ = [\frac{-\tilde{T}_{zz}}{Ac_s^2} - 2\tilde{\Phi}^- - \frac{A}{2pq_p}\widetilde{\Psi}^- + \frac{2pq_s}{A}\widetilde{\Psi}^-][\frac{A^2+4p^2q_sq_p}{2Apq_p}]^{-1}$$
$$(12a)$$

$$\tilde{\Phi}^+ = [A\widetilde{\Psi}^+ + 2pq_p\tilde{\Phi}^- + A\widetilde{\Psi}^-][2pq_p]^{-1}, \qquad (12b)$$

$$A = c_s^{-2} - 2p^2. \qquad (12c)$$

Comparing the composed horizontal and vertical velocity components with the measurements, figure 5, we can see a good match. This means that the ocean floor velocities estimated by the wavefield tomography provided acceptable composition results.

In theory, exact seafloor parameters are required for the composition. To test the sensitivity of the elastic decomposition theory to the seafloor velocities, we performed decomposition on a synthetic data set with a range of velocities. Results showed that velocities with $\pm100 \ m/s$ error are acceptable to a certain extent, figure 6. After that, cross talk starts to contaminate the decomposed results, which makes them not reliable anymore.
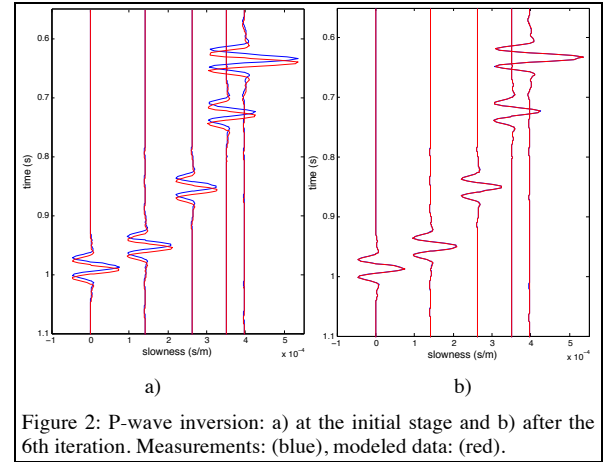

a)   b)

Figure 2: P-wave inversion: a) at the initial stage and b) after the 6th iteration. Measurements: (blue), modeled data: (red).

Conclusions and recommendations

We developed a transmission wavefield tomography scheme to retrieve the P- and S-wave velocities close to the water bottom required for elastic wavefield decomposition. The inversion takes place between a specific depth level below the ocean bottom and the bottom itself. The methodology showed its ability to retrieve a smooth version of the near-bottom velocities. Using the estimated ocean floor P- and S-wave velocities along with an expression of the down-going potentials, we compose the modeled two-way velocity components. This provided good composition results, even

Wavefield Tomography for Elastic Decomposition

though the estimated velocities of the ocean floor did not exactly match the true velocities.

The synthetic data results indicate that it will be possible in practice to retrieve the near-bottom velocity model in combination with the optimum decomposition operators. This can be achieved by actually estimating the up-going wavefields and comparing them with the measurements in a more elaborate scheme.

In this case, the estimated velocities should be more accurate since not only transmission effects would be taken into account, but also reflections and perhaps multiples.
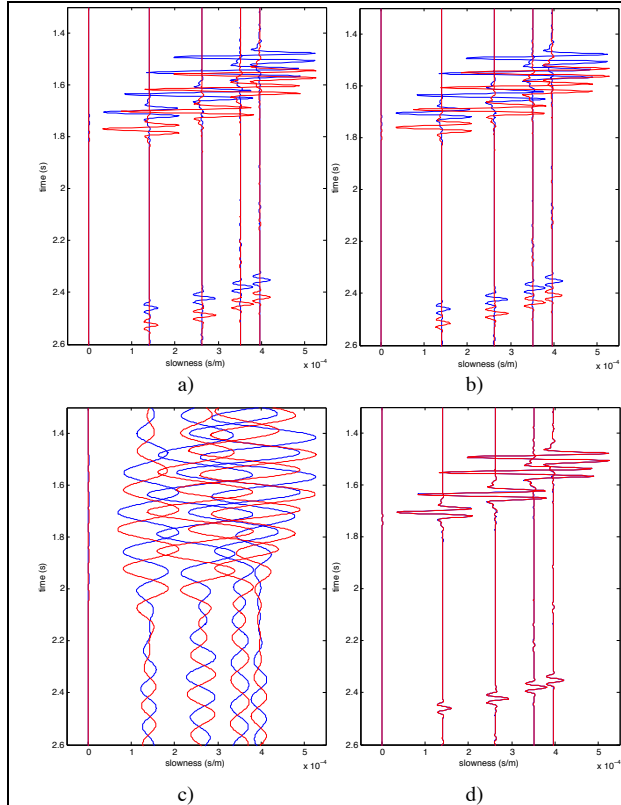
Acknowledgements

a)

b)

c)

d)

Figure 3: S-wave inversion a) at the initial stage, b) after 30 iterations, c) at the initial stage with (5-8) Hz frequency filter and d) after 30 iterations with multi-scale inversion. (Blue): measurements, (red): predicted data.
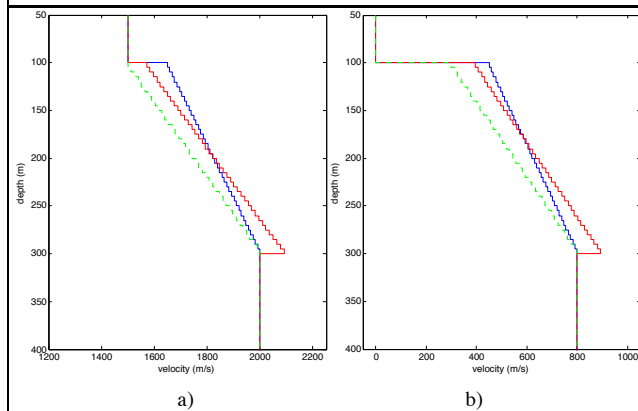

a)

b)

Figure 4: Initial (green), true (blue) and predicted (red): a) P-wave velocity and b) S-wave velocity after multi-scale inversion.
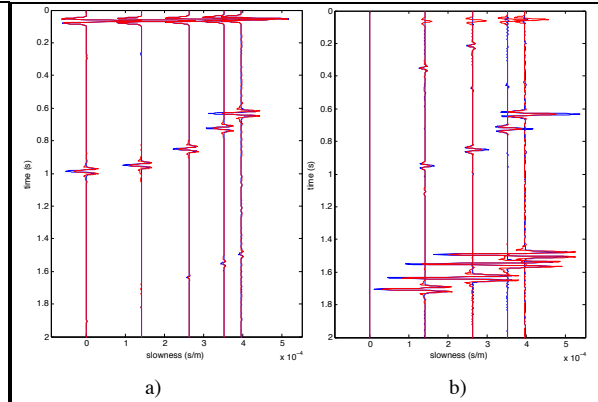

a)

b)

Figure 5: Measurements (blue) and predicted (red): a) vertical velocity component Vz and b) horizontal velocity component Vx.
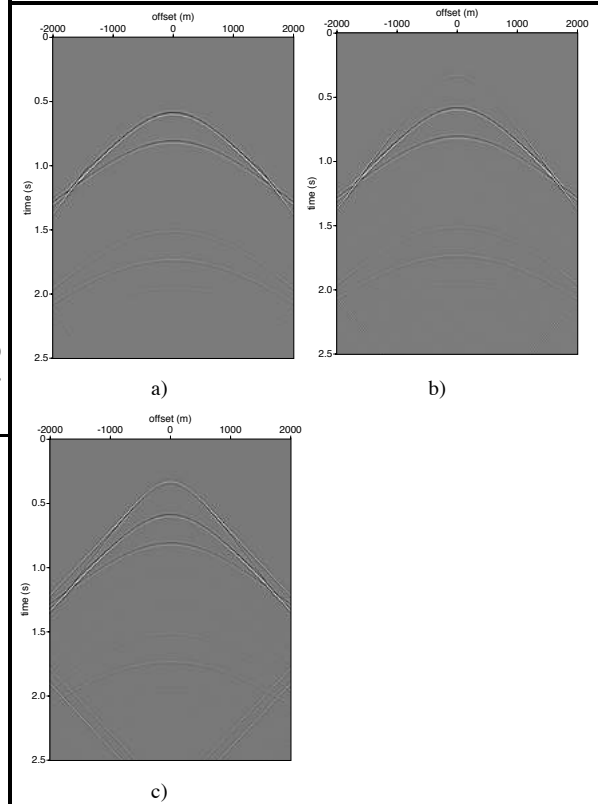

a)

b)

c)

Figure 6: Elastic decomposition to (φ^-) with a) true velocities, $c_p = 1550\ m/s, c_s = 100\ m/s$, and wrong values: b) $c_p = 1650\ m/s, c_s = 200\ m/s$; c) $c_p = 2000\ m/s, c_s = 500\ m/s$.